J Mol Model (2012) 18:5065–5073
DOI 10.1007/s00894-012-1508-y

ORIGINAL PAPER

# *Leishmania donovani* pteridine reductase 1: comparative protein modeling and protein–ligand interaction studies of the leishmanicidal constituents isolated from the fruits of *Piper longum*

**Shakti Sahi · Parul Tewatia · Sabari Ghosal**

Received: 22 April 2012 / Accepted: 14 June 2012 / Published online: 3 July 2012


**Abstract** Visceral leishmaniasis or kala-azar is caused by the dimorphic parasite *Leishmania donovani* in the Indian subcontinent. Treatment options for kala-azar are currently inadequate due to various limitations. Currently, drug discovery for leishmaniases is oriented towards rational drug design; the aim is to identify specific inhibitors that target particular metabolic activities as a possible means of controlling the parasites without affecting the host. *Leishmania* salvages pteridin from its host and reduces it using pteridine reductase 1 (PTR1, EC 1.5.1.33), which makes this reductase an excellent drug target. Recently, we identified six alkamides and one benzenoid compound from the *n*-hexane fraction of the fruit of *Piper longum* that possess potent leishmanicidal activity against promastigotes as well as axenic amastigotes. Based on a homology model derived for recombinant pteridine reductase isolated from a clinical isolate of *L. donovani*, we carried out molecular modeling and docking studies with these compounds to evaluate their binding affinity. A fairly good agreement between experimental data and the results of molecular modeling investigation of the bioactive and inactive compounds was observed. The amide group in the conjugated alkamides and the 3,4-methylenedioxystyrene moiety in the benzenoid compound acts as heads and the long aliphatic chain acts as a tail, thus playing important roles in the binding of the inhibitor to the appropriate position at the active site. The remarkably high activity of a component containing piperine and piperine isomers (3.36:1) as observed by our group prompted us to study the activities of all four isomers of piperine—piperine (2*E*,4*E*), isopiperine (2*Z*,4*E*), isochavicine (2*E*,4*Z*), and chavicine (2*Z*,4*Z*)—against *Ld*PTR1. The maximum inhibitory effect was demonstrated by isochavicine. The identification of these predicted inhibitors of *Ld*PTR1 allowed us to build up a stereoview of the structure of the binding site in relation to activity, affording significant information that should prove useful during the structure-based design of leishmanicidal drugs.

**Keywords** *Piper longum* · Piperaceae · Alkamides · Piperine · *Leishmania donovani* · Molecular docking with *Ld*PTR1

S. Sahi
School of Biotechnology, Gautam Buddha University,
Greater Noida 201308, India

P. Tewatia · S. Ghosal (✉)
Amity Institute of Biotechnology, Amity University,
Sector 125,
Noida 201303, India
e-mail: sabarighosal@gmail.com

S. Ghosal
e-mail: sghosal@amity.edu

## Introduction

Leishmaniases are a broad spectrum of diseases caused by different species of protozoan parasites of the genus *Leishmania*. The most severe clinical form of this disease, visceral leishmaniasis or kala-azar, is caused by the dimorphic parasite *Leishmania donovani* in humans. Most of the drugs that are currently used to treat kala-azar are usually unsatisfactory due to various limitations relating to their route of administration, their unaffordable cost, their toxicity, and the long-term nature of such treatments [1]. In order to expand our arsenal of drugs that can be used for leishmaniasis, new, effective drug targets are urgently required. *Leishmania* is rather unusual in that it salvages pterin from its host. Pteridine reductase 1 (PTR1, EC 1.5.1.33), a broad-spectrum enzyme, is then used by *Leishmania* in pterin (and folate)

metabolism. Since the host of *Leishmania* can synthesize pterin derivatives de novo from GTP but lacks PTR1 activity, PTR1 is considered to be an excellent *Leishmania*-specific drug target [2]. Biochemical studies indicate that NADPH-dependent PTR1 acts as a tetramer and catalyzes the reduction of biopterin to dihydrobiopterin ($H_2B$) and $H_2B$ to tetrahydrobiopterin ($H_4B$). It is also capable of reducing folate to 7,8-dihydrofolate and tetrahydrofolate. PTR1 activity depends on the growth stage of the *L. donovani* promastigote, with high activity observed at the logarithmic stage of the parasite and lower activity (approximately 70% of that seen during the log phase) seen during the stationary phase [3]. The properties of PTR1 suggest that it plays a role in pteridin salvage as well as antifolate resistance. The novelty and possible uniqueness of the pathway in which PTR1 is involved points to the possibility of developing PTR1 inhibitors, which, when used in combination with DHFR (dihydrofolate reductase) inhibitors, could be highly effective against *Leishmania* [4].

Recently, a number of synthetic derivatives of thiones and a few known inhibitors of DHFR, dihydropyridines, and tetrahydropyridines [5–9] have been evaluated for their leishmanicidal activities using a *Ld*PTR1 homology model. Two anticancer agents with a dihydropyrimidine pharmacophore [10] were also docked at the same active site. Various classes of naturally occurring compounds are reported to have antileishmanial activity [11] but, to the best of our knowledge, these compounds have not been virtually screened against the enzyme for pteridin metabolism in *Leishmania*.

*Piper longum* L. (Piperaceae) is widely grown in tropical countries and is used in traditional medicines for tuberculosis, respiratory tract infections, gonorrhea, sleeping problems, chronic pain, and alleviation of anxiety [12]. A large number of physiologically active compounds—esters, amides, alkaloids, lignans, terpenes, chalcones, and flavones—have been isolated from the genus *Piper* [13]. A fresh investigation of the antileishmanial properties of 30 medicinally important plants from an area in which visceral leishmaniasis is endemic—Bihar, India—demonstrated that ethanol extract of *Piper longum* is highly effective against promastigotes and amastigotes of *L. donovani* [14]. Recently, we reported a number of compounds with leishmanicidal activity against promastigotes and axenic amastigotes that were present in an *n*-hexane fraction of *P. longum* [15]. Further investigations in search of new leishmanicidal compounds from the same *n*-hexane fraction resulted in the identification of a component containing piperine and piperine isomers in the ratio 3.36:1 that showed remarkably high activity. Piperine, a major constituent of all *Piper* species, showed comparable leishmanicidal activity to the standard drug pentamidine [16]; however, in comparison to another standard drug, miltefosine, it was completely inactive. Hence, we decided to utilize virtual screening to evaluate the activities of the isolated compounds, making use of our *Ld*PTR1 homology model. Further, the reduced derivatives of abundantly available compounds were evaluated experimentally and by docking them into the same binding pocket.

## Theory and methods

### Chemistry

#### *Plant material and chemical reagents*

Fruits of *Piper longum* were procured from a registered vendor in New Delhi. A voucher specimen (SG/025/2006) was authenticated by Dr. M.P. Sharma, Department of Botany, Hamdard University, New Delhi.

Column chromatography was performed with silica gel 60 (Merck, Mumbai, India), while aluminum sheets (200 μm, 20 × 20 cm) and pre-coated silica gel 60 $GF_{254}$ plates were used for analytical TLC. HPLC was performed on a Waters (Milford, MA, USA) LC system including a 600 pump and a 2998 photodiode array detector. An RP-18 analytical column (5 μm, 3.9 × 300 mm) and HPLC-grade solvents were used. The spots were visualized under UV light (254 and 366 nm) and then sprayed with Dragendorff's reagent. A miltefosine standard (Sigma; purity≥98%) was used as the positive control. UV, IR, ESIMS, and NMR spectra were recorded on instruments from Shimadzu (Kyoto, Japan), Nicolet (Protégé 460; Waltham, MA, USA), Waters (Micromass 1525 LCT), and Bruker (300/75 MHz instrument), respectively.

#### *Extraction and isolation*

Air-dried fruits of *P. longum* (2.5 kg) were extracted with MeOH–$H_2O$ (9:1, 3.5 L × 3 × 24 h) followed by $H_2O$ (2 L) at room temperature. The concentrated MeOH extract was fractionated into *n*-hexane (3.5 L, 40 g), $CH_2Cl_2$ (3.5 L, 43 g), EtOAc (2.5 L, 32 g), and aqueous (25 g) fractions, respectively. Leishmanicidal screening of these fractions identified the *n*-hexane fraction ($IC_{50}$ 100 μg/mL) as the most potent. Successive chromatography of the *n*-hexane fraction (39 g; 5.7 × 85 cm, silica gel 60) using *n*-hexane and a stepwise gradient of EtOAc afforded nine fractions (F-1 to F-9) by TLC monitoring under UV light and Dragendorff's reagent. Compounds **1**–**7** were isolated from the *n*-hexane fraction using various chromatographic techniques, as previously described by our group [15]. Further, chromatography of the combined F-5 and F-6 fractions afforded a light yellow precipitate of crude piperine in excess. Analysis of the precipitate by RP-HPLC with ACN/$H_2O$ (40:60, 1 mL/min) and comparison of the chromatogram with that reported in the literature [31] showed

that it contained two constituents, piperine (**8a**) and piperine isomers (**8b–8d**), in the ratio 3.36:1.

*Catalytic hydrogenation*

Hydrogenating the abundantly available compounds (**2**, **6** and **7**; 10 mg each in 20 mL EtOAc) with 10 % Pd/C at room temperature (8 h) produced the dihydro derivative of **2**, the tetrahydro derivative of **6**, and the hexahydro derivative of **7**, respectively. The hydrogenated products were purified by chromatography. The structures of the pure compounds and their hydrogenated derivatives were elucidated by ESI-MS, $^{1}H$ and $^{13}C$ NMR spectroscopy and by a comparison of the data with the literature values.

## Biology

*In vitro antileishmanial activity versus promastigote, amastigote, and cell cytotoxicity assay*

*L. donovani* (DD8) promastigotes, axenic amastigotes, and macrophages of the cell line J774A.1 were collected from the Cell Death and Differentiation Laboratory of the National Institute of Immunology, New Delhi. The samples were aseptically dissolved in DMSO and diluted appropriately with the growth medium. The activities of these compounds were tested by modified MTT [3-(4,5-dimethylthiazole-2-yl)-2,5-diphenyltetrazolium bromide] assay [17] against a culture of promastigotes in the logarithmic phase. Additionally, the compounds were screened against an axenic culture of amastigotes in the logarithmic phase (transformed from promastigotes in vitro) [18]. The leishmanicidal effect of each compound was expressed as an $IC_{50}$ value (reduction in cell viability compared to cells in culture medium). A miltefosine standard (Sigma, St. Louis, MO, USA; purity≥98%) was used as the positive control. Cell toxicity was assessed by MTT assay on the mouse macrophage cell line J774A.1 in DMEM medium [19]. The cytotoxicities of all of these compounds at $IC_{50}$ and twice $IC_{50}$ indicated that none of the compounds exhibited >7.5% cytotoxicity at $2 \times IC_{50}$.

## Molecular modeling and docking

*Protein preparation*

In the absence of any experimental three-dimensional (3D) structures for *L. donovani* PTR1 [20], we used an iterative implementation of the Threading ASSEmbly Refinement (I-TASSER) program [21–23] and the *L. major* PTR1 crystal structure as the template. Indeed, two templates [PDB (Protein Data Bank) codes: 2QHX (with 92% identity) and 1E7W (with 90% identity)] of *L. major* PTR1 [24] were actually used by the I-TASSER program to model the protein in 3D. Five models were generated and the best model, which had a confidence score (C-score) of −0.41 and a potential energy of −1197.47 kcal $mol^{-1}$, was selected for further study. The C-score is a measure of the quality of the predicted model. Further refinement (to alleviate steric clashes) of the predicted structure was done by performing energy minimization with the optimized potentials for liquid simulations 2005 (OPLS 2005) force field. Minimization was performed until the average root mean square deviation of nonhydrogen atoms reached 0.3 Å. PROCHECK [25] was used for stereochemical analysis of the predicted structure. Further, secondary structural information for the protein was generated by PDBsum [26]. Finally, the 3D model of PTR1 was modified using the protein preparation workflow in the Maestro interface in order to add *N*-acetyl and *N*-methyl amide capping groups to the N-terminus and C-terminus, respectively.

*Ligand structure prediction*

In preparation for the molecular docking simulation, the structure of each isolated compound was built by using the Build module of Schrodinger. The resulting geometries were optimized by molecular mechanics using IMPACT in a dynamic environment using the standard TIP4P water model. Energy minimization was done using the same parameters that were applied for the protein. An RMS gradient of 0.01 was used as the convergence threshold. Ligprep [27] was used to prepare the molecules. Each structure was assigned an appropriate bond order and the charges of the compounds were neutralized. The protonation and tautomeric states of the ligands were then expanded at 7.0±2.0 pH. The resulting geometries were optimized by the OPLS 2005 force field.

*Docking studies and estimation of the binding affinities of naturally occurring compounds and hydrogenated derivatives*

Previous studies have shown that, after binding with co-factor NADPH, PTR1 exhibits much stronger affinities for substrates as well as inhibitors [28]. Hence, the PTR1 model was first docked with co-factor NADPH. All docking studies were carried out using the extra precision (XP) method of GLIDE (grid-based ligand docking with energetics), which examines the complementarities of ligand–receptor interactions using a grid-based method based on the empirical ChemScore function for flexible ligand docking [29]. The centroid of the selected active site residues were used for receptor grid generation during docking as well as blind docking. One thousand docked poses per compound were generated for each of the different conformations of a compound. The complexes, poses, and binding affinities

between the receptor and ligands were analyzed using Schrodinger's suite. All molecular modeling work was performed in Schrodinger Maestro, and binding affinities with the receptor were compared using Ligplot.

## Results and discussion

Bioassay-directed fractionation of the *n*-hexane fraction of *P. longum* afforded seven compounds, namely piperlongumide (**1**) [*N*-isobutyl-19-(3′,4′-methylenedioxyphenyl)-2*E*,4*E* nonadecadienamide], 1-(3,4-methylenedioxyphenyl)-1*E* tetradecene (**2**), piperlongimin A [2*E*-*N*-isobutyl-hexadecenamide] (**3**), 2*E*,4*E*-*N*-isobutyl-octadecenamide (**4**), piperlongimin B [2*E*-octadecenoylpiperidine] (**5**), 2*E*,4*E*-*N*-isobutyl-dodecenamide (**6**), and 2*E*,4*E*,12*E*,13-(3,4-methylenedioxyphenyl)-trideca-trienoic acid isobutyl amide (**7**) (Fig. 1), with leishmanicidal activity. In our previous study we reported that the $IC_{50}$ values for compounds **1**–**7** against promastigotes in vitro ranged between 9 and 15 μg/mL. All of the tested compounds displayed significantly higher activity against axenic amastigotes than against promastigotes. Compound **1** emerged as the most potent against promastigotes and amastigotes, with $IC_{50}$ values of 9 μg/mL (19.2 μM) and 2.81 μg/mL (5.9 μM), respectively [15]. Screening of the hydrogenated derivatives

**Fig. 1** Structures of the compounds **1**–**8d** isolated from the active *n*-hexane fraction of *P. longum*

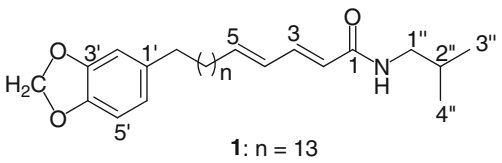


**1**: n = 13

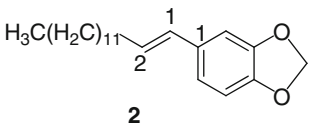


**2**

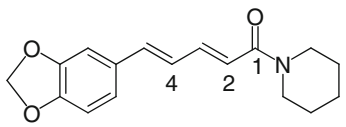


**8a:** 2*E*,4*E*

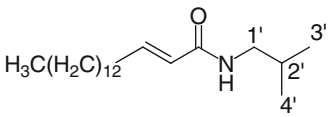


**3**

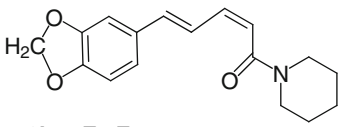


**8b:** 2*Z*,4*E*

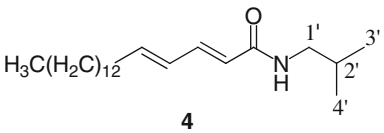


**4**

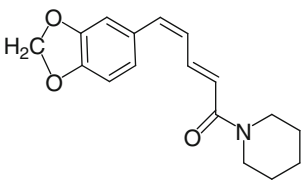


**8c:** 2*E*,4*Z*

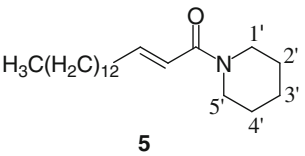


**5**

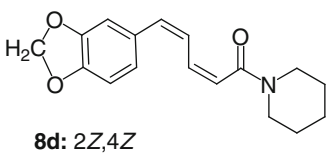


**8d:** 2*Z*,4*Z*

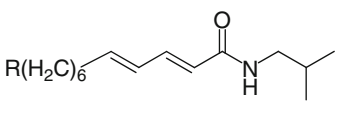


**6**: R = $CH_3$

**7 :** R =

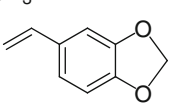

against promastigotes and axenic amastigotes of *L. donovani* showed that they were completely inactive, indicating the prime role played by the conjugated double bonds in the biological activity of these derivatives. In accord with the previous report, we found that piperine (**8a**) was inactive in comparison to the positive control, miltefosine [30], whereas an amorphous form of (crude) piperine exhibited much higher activity, with $IC_{50}$ values of 3.15 and 1.1 μg/mL against promastigotes and axenic amastigotes, respectively (Table 1). Analysis of the crude piperine by RP-HPLC with ACN/$H_2O$ (40:60, 1mL/min) showed that it contained two constituents, **8a** and piperine isomers (**8b–8d**), in the ratio 3.36:1. These two forms were separated by RP-HPLC. However, the $^1H$ NMR spectrum ($CDCl_3$) showed the occurrence of all four isomers, **8a**:**8c**:**8b**:**8d**, in the ratio 2.32:2.23:1.55:1 [31], indicating instantaneous acid-catalyzed isomerization of the piperine isomers in $CDCl_3$. The instability of **8b–8d** became a big constraint on isolating them individually and subsequently checking their biological activities. The cytotoxicities of the active compounds and components, measured at $IC_{50}$ and $2 \times IC_{50}$, showed that none of the compounds exhibited >7.5% cytotoxicity at $2 \times IC_{50}$.

The sequence for *L. donovani* PTR1, comprising 301 amino acids (Fig. 2), was downloaded from the UNIPORT database. Modeling of the 3D structure of the enzyme was performed by the I-TASSER program. The functional enzyme is a tetramer in solution, with each unit comprising seven-stranded β-sheets and ten α-helices, as shown in the ribbon diagram (Fig. 3a). Superimposition of the *Ld*PTR1 model onto the X-ray crystal structure of *L. major* PTR1 (1E7W) showed an average root mean square deviation (RMSD) of 0.723 Å (Fig. 3b). The binding energy of −100.45 and the total energy of −1242.04 kcal $mol^{-1}$ indicated the formation of a fairly stable complex between cofactor NADPH and the *Ld*PTR1 model. Moreover, strong H-bonding interactions were observed between NADPH and His38, Arg39, Tyr37, Ser227, and Arg17 of the protein. The results of the docking studies (Table 2) were in accord with the biological activities exhibited by compounds.

The top-scoring docking pose of compound **1** (−53.47 kcal $mol^{-1}$), one of the most promising compounds, included two major H-bonds between the amide NH and cofactor NADPH (2.154 Å) and between the C-1 ketone carbonyl and the side-chain hydroxyl (1.832 Å) of Tyr114 (Fig. 4), respectively. The isobutyl amide moiety (the "head") enters first, and fits securely inside the narrow gorge formed by Phe113, Met233, Asp232, Arg39, Val127, Asp124, Arg120, Pro117, Gly190, Tyr191, Leu188, Tyr241, Met183, Leu226, and Leu229. In contrast, the top-scoreing docking pose of **7** (−37.39 kcal $mol^{-1}$) displayed only one H-bond between the C-1 ketone carbonyl and the hydroxyl of Tyr191, making the molecule relatively flexible and only loosely associated with *Ld*PTR1. The longer aliphatic linking chain of $(CH_2)_{14}$ of **1** drives the molecule deep inside the pocket, while the shorter alkyl chain of **7** $(CH_2)_6$ leads to less effective penetration. The orientations of the methylenedioxy phenyl moiety in both **1** and **7** probably do not favor any strong interactions at the active site. Compounds **3**, **4**, **5**, and **6** displayed a similar binding mode and almost the same binding interactions as those observed for **7**. Indeed, just as the docking scores were very similar, no significant differences were noted among the biological activities of these compounds. The docking score analysis of **2** (−45.41 kcal $mol^{-1}$) showed that it fits well into the active pocket. The methylenedioxy phenyl moiety of **2** enters the gorge first, establishing strong hydrophobic interactions with Phe113, Arg17, Asp232, Met233, Leu229, Leu226, Tyr241, Leu188, Met183, Gly190, Pro117, Arg190, Tyr114, and Pro115. A major edge-to-face π-stacking interaction with Phe113 as well as a H-bonding interaction with the side chain of Tyr191 and the long hydrophobic chain of $(CH_2)_{11}$ help the molecule to bind firmly into the hydrophobic pocket. This is the first example of a non-nitrogenous inhibitor of *Ld*PTR1 to be reported. In accord with the observed biological activity, all of the reduced derivatives were inactive against the *Ld*PTR1 model, indicating the great importance of the conjugated double bond in the basic skeleton of each molecule.

**Table 1** In vitro leishmanicidal activities of **8a–8d** and the standard miltefosine against promastigotes and axenic amastigotes of *L. donovani*, as well as cell cytotoxicities against the J774A.1 cell line

| Compound | $IC_{50}$±SD (μg/mL) | | Cytotoxicity (%) | |
|---|---|---|---|---|
| | Promastigotes | Amastigotes | At $IC_{50}$±SD [a] | At $2 \times IC_{50}$±SD [a] |
| **8a–8d** | 03.15±0.47 | 1.10±0.09 | 5.05±0.03 | 7.20±0.87 |
| Miltefosine[b] | 08.20±0.36 | 4.37±0.51 | 25.10±0.63 | 37.35±0.03 |

[a] Each compound was examined in a set of triplicate experiments

[b] The compound was used as positive control

* Purity (%) of tested compounds was>90%

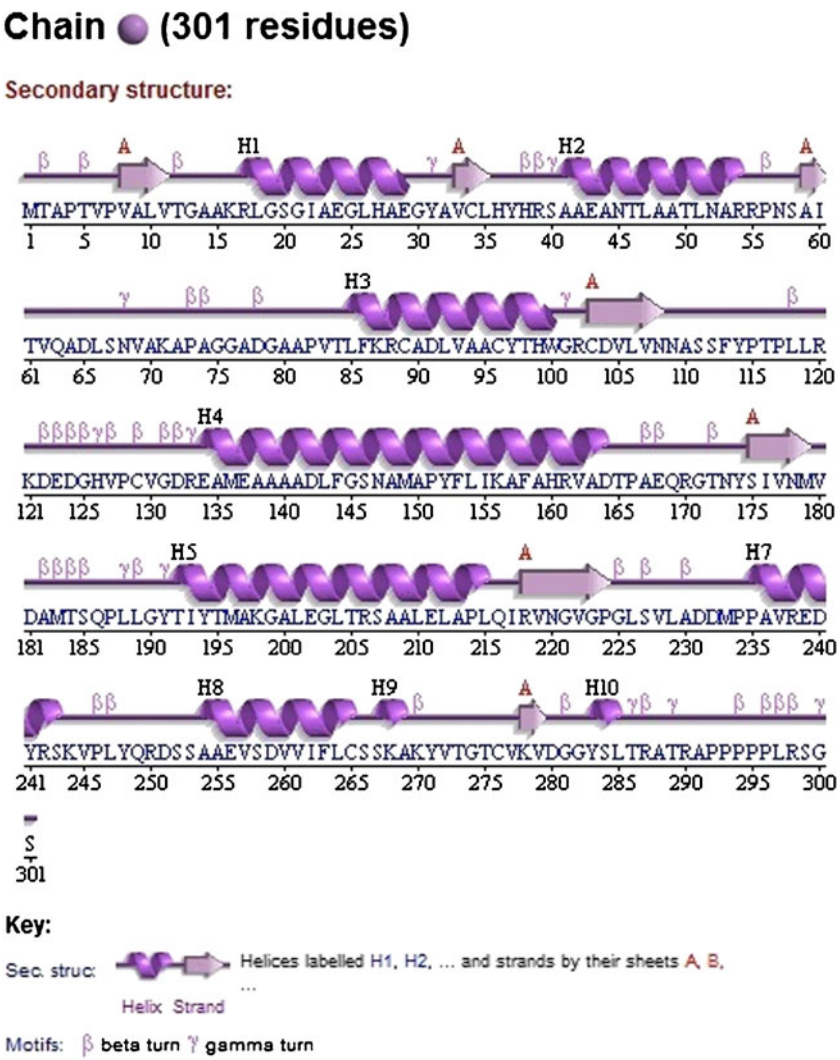


**Fig. 2** Depiction of the secondary structural elements of PTR1, obtained from PDBsum. The secondary structural elements of PTR1 are indicated by *coils* for helices and *arrows* for β-sheets

The surprisingly high activity of crude piperine prompted us to dock individual isomers into the binding pocket. The top-scoring docking pose of each isomer demonstrated that there is a wide variation in binding affinity. The conformational energy of **8c** (56 kcal $mol^{-1}$) was lower than those of **8a** (114 kcal $mol^{-1}$) and **8b** (119 kcal $mol^{-1}$). The docking

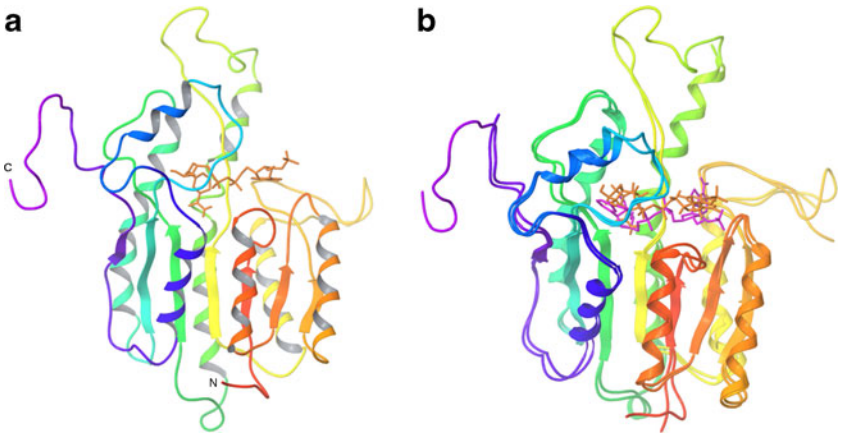


**Fig. 3** **a** Molecular model for *L. donovani* PTR1 derived using coordinates from *L. major* PTR1. Helices (*coils*) and β-sheets (*arrows*) are shown in *different colors*. NADPH is depicted in *orange*. **b** 3D view of the superimposition of the *Ld*PTR1 model on the X-ray crystal structure of *L. major* PTR1 (PDB code 1E7W). NADPH of *Ld*PTR1 and *L. major* PTR1 are shown in *orange* and *purple*, respectively. The diagram shows that there is an average root mean square deviation (RMSD) of 0.723 Å

**Table 2** Molecular docking scores and the residues involved in the interactions of compounds **1**–**8d** with *Ld*PTR1

| Compounds | Docking score | Energy of the model (kcal/mol) | Key interacting residues | |
|---|---|---|---|---|
| | | | Hydrogen bond | Hydrophobic interactions |
| **1** | −5.54 | −53.47 | NADPH , Tyr114 | Phe113, Met233, Asp232, Arg39, Val127, Asp124, Arg120, Pro117, Gly190, Tyr191, Leu188, Tyr241, Met183, Leu226, Leu229 |
| **2** | −5.18 | −45.41 | Tyr191 | Phe113, Arg17, Asp232, Met233, Leu229, Leu226, Tyr241, Leu188, Met183, Gly190, Pro117, Arg190, Tyr114, Pro115 |
| **3** | −3.57 | −36.34 | Arg120 | NADPH, Val127, Pro117, Pro115, Gly190, Tyr191, Leu188, Met183, Leu226, Tyr241, Leu229, Met233, Asp232, Phe113 |
| **4** | −4.82 | −43.1 | Arg120 | NADPH, Phe113, Met183, Tyr241, Leu188, Gly190, Pro117, Tyr191, Pro115, Val127, Asp232, Leu229, Leu226, Arg17 |
| **5** | −4.76 | −41.8 | Arg120 | Phe113, Pro117, Tyr191, Gly190, Val127, Leu188, Met183, Leu226, Leu229, Met233, Asp232, NADPH |
| **6** | −3.86 | −37.01 | Arg120 | NADPH, Phe113, Pro115, Pro117, Tyr191, Gly190, Leu188, Met183, Leu226, Tyr241, Leu229, Met233, Val127 |
| **7** | −4.15 | −37.39 | Phe113, Arg120 | NADPH, Met183, Leu229,Leu226, Tyr241, Asp232, Met233, Tyr114, Tyr191, Gly190, Arg39 |
| **8a** | −4.59 | −26.48 | | NADPH, Phe113, Pro115, Pro117, Val127, Tyr191, Gly190, Met183, Leu226, Met233, Leu229, Asp,232 |
| **8b** | − 4.98 | −28.39 | | NADPH, Tyr241, Leu229, Leu226, Met183, Leu188, Arg17, Met233, Asp232, Phe113, Tyr114 |
| **8c** | −5.55 | −43.89 | Tyr191 | Pro115, Asp232, Leu229, Phe113, Arg 17, Leu226, Met183, Met233, Tyr114, and NADPH. |
| **8d** | −5.15 | −33.51 | | NADPH, Met233, Met183, Leu226, Leu229, Phe113, Leu188, Tyr191, Gly190, Leu189, Arg120 |

score indicated that **8c** participates in strong H-bonding interactions (1.863 Å) with the C-1 ketone carbonyl and the side chain of Tyr191 as well as edge-to-face π-stacking interactions with the methylenedioxy phenyl moiety of the ligand and Phe113 of the protein (Fig. 5), along with major hydrophobic interactions. As the *Ld*PTR1 active site is hydrophobic in nature, the edge-to-face or T-shaped aromatic stacking interactions appear to be crucial to effective inhibition. The ligand resides in the hydrophobic pocket formed by the residues Pro115, Asp232, Leu229, Phe113, Arg17, Leu226, Met183, Met233, Tyr114, and NADPH. On the contrary, the 2*Z* conformation of **8d** does not permit the

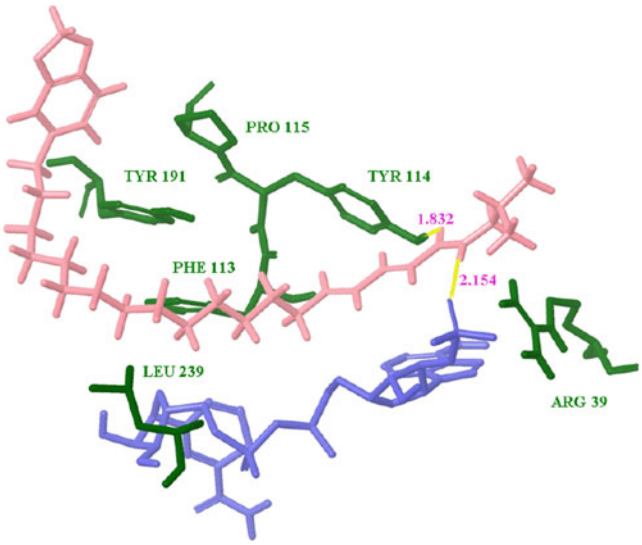


**Fig. 4** The binding mode of compound **1** (shown in *pink*) in the active site of *Ld*PTR1 complexed with cofactor NADPH. The residues of *Ld*PTR1 that are involved in interactions with the ligand are shown in *green*, H-bonding interactions are shown in *yellow*, the relative distances are indicated in *purple*, and NADPH is represented in *blue*

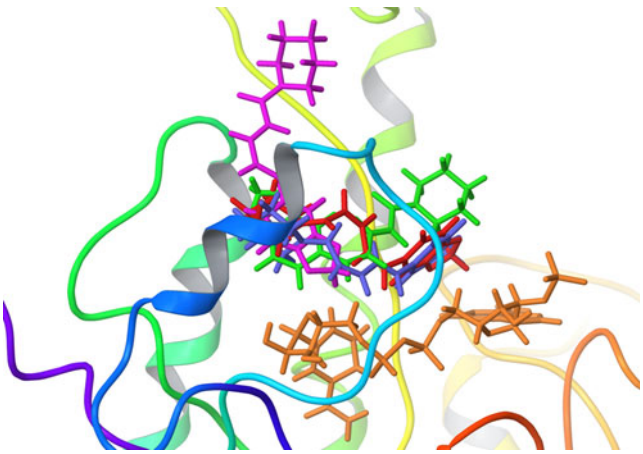

**Fig. 5** 3D views of **8a**–**8d** in the binding pocket of the *Ld*PTR1–NADPH complex. **8a**, **8b**, **8c**, **8d**, and NADPH are shown in *blue*, *purple*, *green*, *pink*, and *orange*, respectively

piperidenamide moiety to participate in any H-bonding interactions or effective edge-to-face π-stacking interactions with the methylenedioxystyrene (*cis*) moiety at the active site. Neither of the top-scoring docking poses of both **8a** and **8b** were stabilized by π–π stacking interactions nor H-bonding. The methylenedioxy phenyl moiety of **8a** experiences serious steric clashes with the protein, leading to decreased hydrophobic interaction and thus negligible biological activity. Hence, it was concluded that **8c** is the most potent *Ld*PTR1 inhibitor. If we extrapolate the results of the docking experiments for the piperine isomers, we can postulate that the remarkably high activity of crude piperine could be due to **8c**. The high specificity of **8c** has stimulated us to plan further in vivo studies to authenticate this promising activity.

## Conclusions

Molecular docking studies revealed that **1** and **8c** are the most promising leishmanicidal compounds, as they show significant binding affinity for *Ld*PTR1. A set of alkamides and a non-nitrogenous benzenoid compound emerged as potential inhibitors of *Ld*PTR1. Further in vivo studies with synthetic derivatives of the naturally occurring lead compounds are recommended in view of the docking results. Additionally, the significant docking result of **8c** could be explored in relation to a number of biological activities that have already been reported for piperine.

**Acknowledgments** The authors acknowledge the Department of Science and Technology and the Council of Scientific and Industrial Research, Government of India, for financial support, and Dr. A.K. Chauhan, Founder President, Amity University, for his continuous encouragement.

**No conflict of interest** None of the authors of the above manuscript has declared any conflict of interest within the last three years which may arise from being named as an author on the manuscript.

## References

1. Rocha LG, Almeida JRGS, Macedo RO, Barbosa-Filho JMA (2005) Review of natural products with antileishmanial activity. Phytomedicine 2:514–535
2. Nichol CA, Smith GK, Duch DS (1985) Biosynthesis and metabolism of tetrahydrobiopterin and molybdopterin. Annu Rev Biochem 42:729–764
3. Cunningham ML, Titus RG, Turco SJ, Beverley SM (2001) Regulation of differentiation to the infective stage of the protozoan parasite *Leishmania major* by tetrahydrobiopterin. Science 292:285–287
4. Bello AR, Nare B, Freedman D, Hardy L, Beverley SM (1994) PTR1: a reductase mediating salvage of oxidized pteridines and methotrexate resistance in the protozoan parasite *Leishmania major*. Proc Natl Acad Sci USA 91:11442–11446
5. Kumar P, Sundar S, Singh N (2007) Degradation of pteridine reductase 1 (PTR1) enzyme during growth phase in the protozoan parasite *Leishmania donovani*. Exp Parasitol 116:182–189
6. Kumar P, Kumar A, Verma SS, Dwivedi N, Singh N, Siddiqi MI, Tripathi RP, Dube A, Singh N (2008) *Leishmania donovani* pteridine reductase 1: biochemical properties and structure-modeling studies. Exp Parasitol 120:73–79
7. Singh N, Kaur J, Kumar P, Gupta S, Singh N, Ghosal A, Dutta A, Kumar A, Tripathi RP, Siddiqi ML, Mandal C, Dube A (2009) An orally effective dihydropyrimidone (DHPM) analogue induces apoptosis-like cell death in clinical isolates of *Leishmania donovani* overexpressing pteridine reductase 1. Parasitol Res 105:1317–1325
8. Kaur J, Singh BK, Tripathi RP, Singh P, Singh N (2009) *Leishmania donovani*: a glycosyl dihydropyridine analogue induces apoptosis like cell death via targeting pteridine reductase 1 in promastigotes. Exp Parasitol 123:258–264
9. Pandey VP, Bisht SS, Mishra M, Kumar A, Siddiqi MI, Verma A, Mittal M, Sane SA, Gupta S, Tripathi RP (2010) Synthesis and molecular docking studies of 1-phenyl-4-glycosyl-dihydropyridines as potent antileishmanial agents. Eur J Med Chem 45:2381–2388
10. Kaur J, Sundar S, Singh N (2010) Molecular docking, structure–activity relationship and biological evaluation of the anticancer drug monastrol as a pteridine reductase inhibitor in a clinical isolate of *Leishmania donovani*. J Antimicrob Chemother 65:1742–1748
11. Chan-Bacab MJ, Pena-Rodriguez LM (2001) Plant natural products with leishmanicidal activity. Nat Prod Rep 18:674–688
12. Kumar S, Arya P, Mukherjee C, Singh BK, Singh N, Parmar VS, Prasad AK, Ghosh B (2005) Novel aromatic ester from *Piper longum* and its analogues inhibit expression of cell adhesion molecules on endothelial cells. Biochemistry 44(48):15944–15952
13. Parmar VS, Jain SC, Bisht KS, Jain R, Taneja P, Jha A, Tyagi OD, Prasad AK, Wengel J, Olsen CE, Boll PM (1997) Phytochemistry of the genus *Piper*. Phytochemistry 4:597–603
14. Singh SK, Bimal S, Narayan S, Jee E, Bimal D, Das P, Bimal R (2011) *Leishmania donovani*: assesment of leishmanicidal effects of herbal extracts obtained from plants in the visceral leishmaniasis endemic area of Bihar. India Exp Parasitol 127:552–558
15. Ghosal S, Deb A, Mishra P, Vishwakarma R (2012) Leishmanicidal compounds from the fruits of *Piper longum*. Planta Med 78:906–908
16. Kapil A (1993) Piperine, a potent inhibitor of *Leishmania donovani* promastigotes in vitro. Planta Med 59:475
17. Dutta A, Bandopadhyay S, Mandal C, Chatterjee M (2005) Development of a modified MTT assay for screening antimonial resistant field isolates of Indian visceral leishmaniasis. Parasitol Int 54:119–122
18. Pan AA, Duboise SM, Eperon S, Rivas L, Hodgkinson V, Ttraub-Cseko Y, Mcmohan-Pratt D (1993) Developmental life cycle of leishmania-cultivation and characterization of cultured extracellular amastigotes. J Eukaryot Microbiol 40:213–223
19. Manandhar KD, Jadav TP, Prajapati VK, Kumar S, Rai M, Dube A, Srivastava ON, Sundar S (2008) Antileishmanial activity of nano-amphotericine B deoxycholate. J Antimicrob Chemother 62:376–380
20. Jain E, Bairoch A, Duvaud S, Phan I, Redaschi N, Suzek BE, Martin MJ, McGarvey P, Gasteiger E (2009) Infrastructure for the life sciences: design and implementation of the UniProt website. BMC Bioinforma 10:136
21. Wu S, Skolnick J, Zhang Y (2007) Ab Initio modeling of small proteins by iterative Tasser simulations. BMC Biol 5:17
22. Zhang Y (2007) Template based modeling and free modeling by I-TASSER in CASP7. Proteins 8:108–117
23. Zhang Y (2008) I-TASSER server for protein 3D structure prediction. BMC Bioinforma 9:40

24. Gourley DG, Schuttelkopf A, Leonard G, Luba J, Hardy L, Beverley S, Hunter WN (2001) Pteridine reductase mechanism correlates pterin metabolism with drug resistance in trypanosomatid parasites. Nat Struct Biol 8:521–525
25. Laskowski RA, MacArthur MW, Moss DS, Thornton JM (1993) PROCHECK—a program to check the stereochemical quality of protein structures. J App Cryst 26:283–291
26. Laskowski RA (2009) PDBsum new things. Nucleic Acids Res 37: D355–359
27. Schrödinger, LLC (2009) LigPrep, version 2.3. Schrödinger, LLC, New York
28. Nare B, Luba J, Hardy LW, Beverly SM (1997) The roles of pteridine reductase 1 and dihydrofolate reductase–thymidylate synthase in pteridine metabolism in the protozoan parasite *Leishmania major*. J Biol Chem 272:13883–13891
29. Friesner RA, Banks JL, Murphy RB, Halgren TA, Klicic JJ, Mainz DT, Repasky MP, Knoll EH, Shelley M, Perry JK, Shaw DE, Francis P, Shenkin PS (2004) Glide: a new approach for rapid, accurate docking and scoring. 1. Method and assessment of docking accuracy. J Med Chem 47:1739–1749
30. Singh PI, Jain SK, Kaur A, Singh S, Kumar R, Grag P, Sharma SS, Arora SK (2011) Synthesis and antileishmanial activity of piperoyl-amino acid conjugates. Eur J Med Chem 45:3439–3445
31. Hashimato H, Yaoi T, Hiroyuki K, Yoshida T, Maoka T, Fujiwara Y, Yamamoto Y, Mori K (1996) Photochemical isomerization of piperine, a pungent constituent in pepper. Food Sci Technol Int 2:24–29